Separation Science and Technology
Publication details, including instructions for authors and subscription information:
http://www.informaworld.com/smpp/title~content=t713708471

Adsorption of carbon dioxide, methane, and nitrogen: pure and binary mixture adsorption by ZSM-5 with SiO_2/Al_2O_3 ratio of 30

P. J. E. Harlick[a]; F. H. Tezel[a]
[a] Department of Chemical Engineering, Univerisity of Ottawa, Ottawa, Canada

Online publication date: 25 April 2002

To cite this Article Harlick, P. J. E. and Tezel, F. H.(2002) 'Adsorption of carbon dioxide, methane, and nitrogen: pure and binary mixture adsorption by ZSM-5 with SiO_2/Al_2O_3 ratio of 30', Separation Science and Technology, 37: 1, 33 — 60
To link to this Article: DOI: 10.1081/SS-120000320
URL: http://dx.doi.org/10.1081/SS-120000320

SEPARATION SCIENCE AND TECHNOLOGY, 37(1), 33–60 (2002)

ADSORPTION OF CARBON DIOXIDE, METHANE, AND NITROGEN: PURE AND BINARY MIXTURE ADSORPTION BY ZSM-5 WITH SiO_2/Al_2O_3 RATIO OF 30

P. J. E. Harlick and F. H. Tezel*

Department of Chemical Engineering, University of Ottawa, Ottawa, Ontario, Canada

ABSTRACT

The adsorption of binary gas mixtures of CO_2-N_2, CO_2-CH_4, and CH_4-N_2 were studied by using H-ZSM-5 as the adsorbent with a SiO_2/Al_2O_3 ratio of 30. Pure isotherms for N_2 and CH_4 at 40°C and CH_4-N_2 binary isotherms at 40°C and 1.0 atm total pressure have been determined using concentration pulse chromatography. For CO_2-N_2 and CO_2-CH_4 pure and binary systems, previously published data were used. The applicability of the binary adsorption prediction models, Extended Langmuir, Extended Nitta, Ideal Adsorbed Solution Theory, and the Flory–Huggins form of the Vacancy Solution Theory have been studied.

The CH_4-N_2 binary isotherms exhibit behavior similar to the pure component isotherms, with CH_4 as the dominant adsorbate. The separation factor steadily declines as the mole fraction of CH_4 in the gas phase is increased.

All the theoretical models used reasonably predict the binary systems for CH_4-N_2. The CO_2-N_2 system was not predicted

*Corresponding author. E-mail: tezel@eng.uottawa.ca

well. CO_2-CH_4 behavior was predicted reasonably well by all the models, except by the Extended Nitta. The models appear to be able to predict systems where the adsorption capacities of each component are relatively similar.

Key Words: Adsorption; Equilibrium; Binary adsorption isotherms; Multi-component adsorption; Carbon dioxide; Nitrogen; Methane; ZSM-5; HT-CPM; Extended Langmuir; IAST; FH-VST

Abbreviations: CPM, Concentration pulse method; EL, Extended Langmuir; FH-VST, Flory–Huggins vacancy solution theory; GC, Gas chromatograph; HT-CPM, Harlick–Tezel concentration pulse method; IAST, Ideal adsorbed solution theory; MFC, Mass flow controller; SSR, Sum of square residuals; TCD, Thermal conductivity dectector; VST, Vacancy solution theory

INTRODUCTION

The use of adsorption based gas separations for industrial processes are widespread. The developments of new adsorbents for these separations are also evolving rapidly. This growth facilitates the need to characterize the adsorbents for a very large subset of gases (1). One dynamic method of analysis is by using the chromatographic technique. This method can be employed in several ways: tracer gas, step change, and pulse chromatography. In this study, concentration pulse chromatography has been employed (2–5).

The use of concentration pulse chromatography for adsorbent screening is very attractive since it is relatively inexpensive to set up. Further, this method is capable of characterizing adsorbents quicker than other methods presently used. However, presently available methods for determining binary isotherms from concentration pulse method (CPM) data for highly selective adsorbents are not applicable (6). A novel solution method for determining binary isotherms from concentration pulse chromatography data, the Harlick–Tezel Concentration Pulse Method (HT-CPM), was shown in our earlier work (7). This method proved to be able to handle binary adsorption systems where the components exhibit large differences in capacity. Further, this method was described to be able to incorporate any functional form that can fit the experimental data. This attribute makes this method more versatile than the polynomial or the functional form developed by authors in Ref. (8). Therefore, in this study, the HT-CPM was used for determining the CH_4-N_2 binary isotherms with H-ZSM-5-30 (H-ZSM-5 with SiO_2/Al_2O_3 ratio of 30). The results are compared to three binary predictive models, Extended Langmuir, Ideal Adsorbed Solution Theory, and Flory–

MARCEL DEKKER, INC.
270 Madison Avenue, New York, New York 10016

Huggins form of the Vacancy Solution Theory. The CO_2-CH_4 and CO_2-N_2 binary systems with H-ZSM-5-30, shown in our previous studies (7), are also given and compared with the predictions given by the previously mentioned models.

BACKGROUND AND LITERATURE REVIEW

With concentration pulse method (CPM), a pulse of sample is injected into the carrier gas stream and passes through an adsorbent packed column. The response of the column to the injection is measured as concentration vs. time at the exit of the column. From this response peak a mean retention time of the sample, μ, is determined experimentally:

$$\mu = \frac{\int_0^\infty c(t-\mu_D)\mathrm{d}t}{\int_0^\infty c\mathrm{d}t} \tag{1}$$

The term μ_D is the mean dead time. This dead time is the measure of the time required for a sample pulse to travel through the empty volume of the interconnecting tubing from injection point to the detector, and void space in the packed column.

At that carrier gas composition the mean retention time is related to the effective isotherm slope, K, by Eq. (2) (2–9):

$$\mu = \frac{L}{v}\left[1 + \frac{(1-\varepsilon)}{\varepsilon}K\right] \tag{2}$$

$$K_\mathrm{p}(\text{Dimensional}) = K(\text{Dimensionless}) \times \text{CF}$$

The system dependent constant CF is the conversion factor for transforming the dimensionless K to the dimensional K_p. The K_p value is related to the slopes of the isotherms of the components in the carrier gas mixture. For a binary mixture, the relationship is given as follows:

$$K_\mathrm{p}(\text{Experimental}) = (1-y_1)\frac{\mathrm{d}q_1}{\mathrm{d}P_1} + y_1\frac{\mathrm{d}q_2}{\mathrm{d}P_2} \tag{3}$$

Where, (dq_1/dP_1) and (dq_2/dP_2) are the slopes of the adsorption isotherms for components 1 and 2, respectively.

This method allows for the experimental evaluation of both pure and binary mixture isotherms when K_p values are determined for different concentrations of the carrier gas. The interpretation for pure isotherms is performed if the second

component in the carrier gas mixture is not appreciably adsorbed, for example when helium (He) is used. This results with (dq_2/dP_2) in the second term of Eq. (3) being constant, D:

$$K_p(\text{Experimental}) = (1 - y_1)\frac{dq_1}{dP_1} + y_1 D \tag{4}$$

The value of D is determined from the limiting value of K_p as y_1 approaches 1. The pure component isotherm is then obtained by integrating Eq. (4) with the value of K_p determined for different concentrations of the carrier gas from Eqs. (1) and (2) (2,4–13).

For binary isotherms, both components in the mixed carrier gas are adsorbed and (dq_2/dP_2) in the last term of Eq. (3) is not constant. The experimental K_p data represent the combined contribution of both components. The procedure for evaluating binary isotherms according to the HT-CPM (Harlick and Tezel-Concentration Pulse Method) is generally performed by fitting the K_p vs. mole fraction (y_1) data to a function of i parameters:

$$K_p(\text{Experimental}) = f(A_i, y_1) \tag{5}$$

Provided this functional form fits the data well, the isotherm slope functions are derived from $f(A_i, y_1)$ with unknown parameters, B_i and C_i, as follows:

$$\frac{dq_1}{dP_1} = \frac{df(A_i, y_1)}{dy_1} = g(B_i, y_1) \tag{6}$$

$$\frac{dq_2}{dP_2} = \frac{df(A_i, y_1)}{dy_1} = h(C_i, y_1) \tag{7}$$

The isotherms are found by the integration of Eqs. (6) and (7).

$$q_1 = \int g(B_i, y_1)\, dP_1 \tag{8}$$

$$q_2 = \int h(C_i, y_1)\, dP_2 \tag{9}$$

Note: $P_1 = P_{\text{Total}} y_1$, $P_2 = P_{\text{Total}}(1 - y_1)$. When Eqs. (6) and (7) are substituted into Eq. (3), the following $K_p(B_i, C_i, y_1)$ relationship is derived:

$$K_p(\text{Experimental}) = (1 - y_1)[g(B_i, y_1)] + y_1[h(C_i, y_1)] \tag{10}$$

MARCEL DEKKER, INC.
270 Madison Avenue, New York, New York 10016

The values of the B_i and C_i parameters are found by minimizing the following objective function:

$$SSR = \sum_{y_1=y_{\min}}^{y_1=y_{\max}} \{K_p[\text{Experimental}] - ((1 - y_1)(g[B_i, y_1]) + y_1(h[C_i, y_1]))\}^2 \quad (11)$$

In our earlier paper (6) we have noted that the minimization of Eq. (11) could not be performed with only the data, since a number of solutions would exist. The following constraints were imposed on the system, in order to ensure that the solution reflects what is physically occurring.

(1) The end-points of the binary isotherms must coincide with the pure isotherms:

$$q_1(\text{Binary})|_{y_1=1} = q_1(\text{Pure})|_{P_{\text{Total}}} \quad (12)$$

$$q_2(\text{Binary})|_{y_1=0} = q_2(\text{Pure})|_{P_{\text{Total}}} \quad (13)$$

(2) If the adsorbates are similar in properties, especially at low surface coverage (θ), the isotherm slopes must also be set greater than or equal to zero across the entire range of y_1 (i.e. no maximum should be exhibited by the isotherms) (14):

$$\frac{dq_1}{dP_1} \geq 0 \quad \text{and} \quad \frac{dq_2}{dP_2} \geq 0 \quad (14)$$

(3) The K_p function should pass through the experimental binary K_p data at $y_1 = 0$ and $y_1 = y_1(\max)$:

$$K_p(\text{Experimental})|_{y_1=0} = K_p(\text{equation 10})|_{y_1=0} \quad (15)$$

$$K_p(\text{Experimental})|_{y_1\to 1} = K_p(\text{equation 10})|_{y_1\to 1} \quad (16)$$

By using these constraints (Eqs. (12)–(16)) to bind the objective function (Eq. (11)) a constrained non-linear regression is performed to determine the B_i and C_i parameters and thus determine the binary isotherms. The regressed K_p curve is given by Eq. (10) and the binary isotherms are given by Eqs. (8) and (9). The applicability of the HT-CPM has been shown with CO_2–N_2 and CO_2–CH_4 binary adsorption systems using H-ZSM-5 with SiO_2/Al_2O_3 ratios of 30 and 280 (6,7,9), where other methods are not capable of producing feasible results.

MARCEL DEKKER, INC.
270 Madison Avenue, New York, New York 10016

In this study, the 5-parameter function that was proposed in our previous work (7) was used which is defined as follows:

$$K_{\mathrm{p}} = A_1 + A_2 y_1 + A_3 y_1^2 + A_4 \ln(|y_1 + \lambda|) \tag{17}$$

where $\lambda \neq 0$.

The corresponding isotherm slope functions are:

$$\frac{\mathrm{d}q_1}{\mathrm{d}P_1} = g(B_i, y_1) = B_1 + 2B_2 y_1 + \frac{B_3}{(|y_1 + \lambda|)} \tag{18}$$

$$\frac{\mathrm{d}q_2}{\mathrm{d}P_2} = h(C_i, y_1) = C_1 + 2C_2 y_1 + \frac{C_3}{(|y_1 + \lambda|)} \tag{19}$$

Integration of Eqs. (18) and (19) results in following binary isotherm equations:

$$q_1 = \left\{ B_1 y_1 + B_2 y_1^2 + B_3 \ln\left(\left| \frac{y_1 + \lambda}{\lambda} \right| \right) \right\} P \tag{20}$$

$$q_2 = \left\{ C_1(1 - y_1) + C_2(1 - y_1^2) - C_3 \ln\left(\left| \frac{y_1 + \lambda}{1 + \lambda} \right| \right) \right\} P \tag{21}$$

When Eqs. (18) and (19) are substituted into Eq. (10), following equation is obtained:

$$K_{\mathrm{p}}(\mathrm{Experimental}) = (1 - y_1)\left[B_1 + 2B_2 y_1 + \frac{B_3}{(|y_1 + \lambda|)} \right] + y_1 \left[C_1 + 2C_2 y_1 + \frac{C_3}{(|y_1 + \lambda|)} \right] \tag{22}$$

This equation is then used to define the objective function as follows:

$$SSR = \sum_{y_1 = y_{\min}}^{y_1 = y_{\max}} \left\{ K_p[\mathrm{Exp}] - \left((1 - y_1)\left[B_1 + 2B_2 y_1 + \frac{B_3}{(|y_1 + \lambda|)} \right] + y_1 \left[C_1 + 2C_2 y_1 + \frac{C_3}{(|y_1 + \lambda|)} \right] \right) \right\}^2 \tag{23}$$

This objective function is minimized within the bounds of the constraints given by Eqs. (12)–(16) to determine the unknown B_i and C_i parameters. These parameters are then used in Eqs. (20) and (21) for the calculation of the binary isotherms and in Eq. (22) for the regressed K_{p} curve. This method of determining binary isotherms (HT-CPM) has been compared with other CPM methods, as well as more directly measured binary isotherms (9). For the binary systems

where the two adsorbates have similar adsorption capacities, all the CPM's did well compared to the other directly measured experimental binary isotherms. But for the binary systems where the adsorption properties of the two adsorbates are quite different, HT-CPM was shown to be superior to other CPM's.

After determining the binary isotherms, the equilibrium separation factor defined by Eq. (24) can be calculated and plotted against y_1.

$$\alpha_{12} = \frac{x_1/y_1}{x_2/y_2} \tag{24}$$

The characteristic separation factor curve for the binary system can be studied.

THEORETICAL MODELS

The theoretical models used in this study were the Extended Langmuir (EL), Extended Nitta (Nitta), Ideal Adsorbed Solution Theory (IAST), and the Flory–Huggins form of the Vacancy Solution Theory (FH-VST). Each of these theoretical models uses different assumptions for the prediction of the binary adsorption system. A description of the Extended Langmuir model is given in Refs. (15,16). Extended Nitta model has been discussed in Refs. (17,18). The IAST is given in Ref. (19). The FH-VST, which uses the Flory–Huggins activity coefficients, is given in Refs. (20–23). The pure isotherm equations used to fit the pure component data are given as follows:

$$\text{Langmuir}: \quad q = \frac{q_{\mathrm{m}} BP}{1 + BP} \tag{25}$$

$$\text{Freundlich}: \quad q = bP^{(1/n)} \tag{26}$$

$$\text{FH–VST}: \quad P = \frac{q_m^{\infty}}{b}\left(\frac{\theta}{1-\theta}\right)\exp\left(\frac{\alpha_{1v}^2\theta}{1+\alpha_{1v}\theta}\right) \tag{27}$$

$$\text{Nitta}: \quad BP = \frac{(q/q_{\mathrm{m}})}{\left[1-\left(\frac{q}{q_{\mathrm{m}}}\right)\right]^a} \tag{28}$$

There is an abundance of pure component adsorption data, whereas the experimental binary data is deficient in the literature. When experimental binary adsorption data are available, examination of the predicted binary systems from the pure component data will uncover the best-suited model. This will enable the most accurate model to be suggested for future use with similar binary adsorption systems.

MARCEL DEKKER, INC.
270 Madison Avenue, New York, New York 10016

OBJECTIVE

The purpose of this study was to determine the CH_4-N_2 binary isotherms using H-ZSM-5-30 as the adsorbent. Further, the applicability of the EL, Nitta, IAST, and FH-VST models for predicting the binary system behavior was studied. Pure and binary isotherms, $x-y$ phase diagrams, and the separation factor plots are given for the CH_4-N_2 binary system. Previously determined CO_2-N_2 and CO_2-CH_4 binary isotherms and $x-y$ adsorption phase diagrams (7) are given and compared with the theoretical models for each of the binary systems studied.

EXPERIMENTAL

A schematic diagram of the experimental apparatus is shown in Fig. 1. The details of the gases used are given in Table 1. The experimental and column characteristics are given in Table 2.

As shown in Fig. 1, the flowrates and mixing of the gases (A) were controlled by a series of MKS mass flow controllers (MFC), model numbers 1359 (0–50 sccm range), and set to a total flowrate of 40 cc/min at 40°C. A mixing chamber (B) was installed after the MFC's to ensure a homogeneous mixture in the carrier gas. A thermal conductivity detector (TCD) with a GOW-MAC power supply (C) was placed after the mixing chamber to measure the composition of the carrier gas and thus ensure mixture stability. The carrier gas was then passed

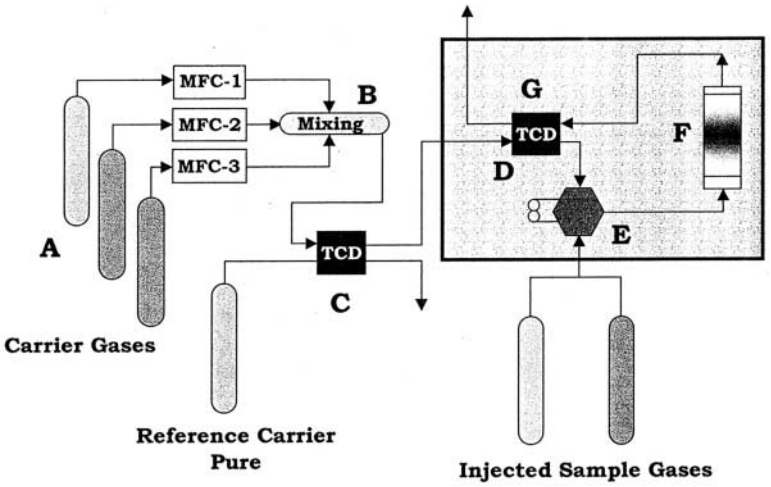

Figure 1. Schematic diagram of the experimental apparatus.

MARCEL DEKKER, INC.
270 Madison Avenue, New York, New York 10016

Table 1. Gases Used in Pure and Binary Adsorption Runs

Type	Grade	Purity (%)	Supplier
He	Ultra pure carrier	99.998	Air products
CO_2	Research	99.995	Air products
CH_4	CP	99.5	Air products
N_2	Ultra high purity	99.999	Air products

through the reference side of the TCD in the GC (D). This TCD was used to measure the response of the column to the sample injection (E). After the injection, the carrier and sample passed through the packed column (F) and the response was measured (G).

Data acquisition was performed using National Instruments based data acquisition card and Labview v5.0 on an Intel based computer. Each column was independently packed with H-ZSM-5 adsorbent and was contained within a Varian 3400 gas chromatograph at 40°C. The GC was equipped with a high sensitivity thermal conductivity detector.

Before the start of each experimental run, the adsorbent was regenerated at 1.0 atm total pressure and 350°C under a 40 sccm helium purge, for approximately 12 hr.

In order to determine the system dead time, a helium injection into the nitrogen carrier was used. The regenerated adsorbent packed column was then

Table 2. Experimental and Column Specifications

Particle Mesh Size	20–60
Average particle diameter	545 μm
% Binder (wt)	16.5
Bed porosity	0.382
Column length	24.75 cm
Column inner diameter	0.45 cm
Total flowrate	40.0 cc/min @ 40°C
Total pressure	1.0 Atm.
Temperature	40.0°C
Regeneration temperature	350°C
Regeneration pressure	1.0 Atm.
Regeneration time	12 hr

allowed to reach equilibrium with the N_2 carrier. The equilibrium state was confirmed by noting the response of the detector. The TCD operates on a wheat-stone bridge principle. Therefore, a steady baseline would indicate that the composition and flowrate of the influent was equal to the effluent. Next, an injection of He was made. Helium gas was used since it is non-adsorbing. This property allows for an accurate measure of the time required for the pulse to travel through the void space of the tubing and the adsorbent packed column.

When determining binary isotherms mixed carriers were used without the He gas. For the CH_4–N_2 system, N_2 was used as the primary gas. Samples of each gas were injected into the column at different carrier gas concentrations.

It is important to note that the experimental data represents binary isotherm's effective slope at a particular mixture composition. As the injection volume approaches zero, the K_p values found by both injections should be identical. When CH_4 is injected, the mixture composition increases slightly in CH_4 concentration. When N_2 is injected, the mixture composition decreases slightly in CH_4 concentration. Therefore, both adsorbates are injected into the mixed carrier gas and the average K_p was found. For this study, a 0.25 cc sample loop was used.

ADSORBENTS–ADSORBATES

The adsorbent used in this study was H-ZSM-5 with silica to alumina (SiO_2/Al_2O_3) ratio of 30, which was prepared and donated by Dr Ahmet Sirkecioglu, from the Department of Chemical Engineering at Istanbul Technical University in Istanbul, Turkey. It was supplied in powder form, which is not appropriate for use with the CPM, since a large pressure drop and possible adsorbent loss due to flow would be encountered. Therefore, the adsorbent powder was combined with a Kaolin binder. A 16.5 wt% binder was used in order to maintain sufficiently high enough pellet strength when exposed to the conditions of the experiments. All the results given in this work are corrected with respect to the 16.5 wt% binder and therefore represent properties of the pure ZSM-5 without the binder.

The H-ZSM-5 adsorbent is a pentasil zeolite with the silicalite structure. The crystalline structure consists of eight double 5-member rings built around two double 6-member rings forming a double 10-membered ring unit cell. These 10-membered rings combine to form the lattice structure, which in turn combine to form the crystalline structure (24,25).

The adsorbates examined in this study were CO_2, CH_4 and N_2. A summary of some of the properties of these adsorbates is given in Table 3.

Marcel Dekker, Inc.
270 Madison Avenue, New York, New York 10016

Table 3. Adsorbate Properties[a]

Adsorbate	Property				
	Molecular Weight	Kinetic Diameter (Å)	Dipole Moment $\times 10^{18}$ (esu cm)	Quadrupole Moment $\times 10^{26}$ (esu cm^2)	Polarizability $\times 10^{25}$ (cm^3)
CO_2	44	3.30	0	4.30	26.5
N_2	28	3.64	0	1.52	17.6
CH_4	16	3.80	0	0	26.0

[a] See Ref. (27).

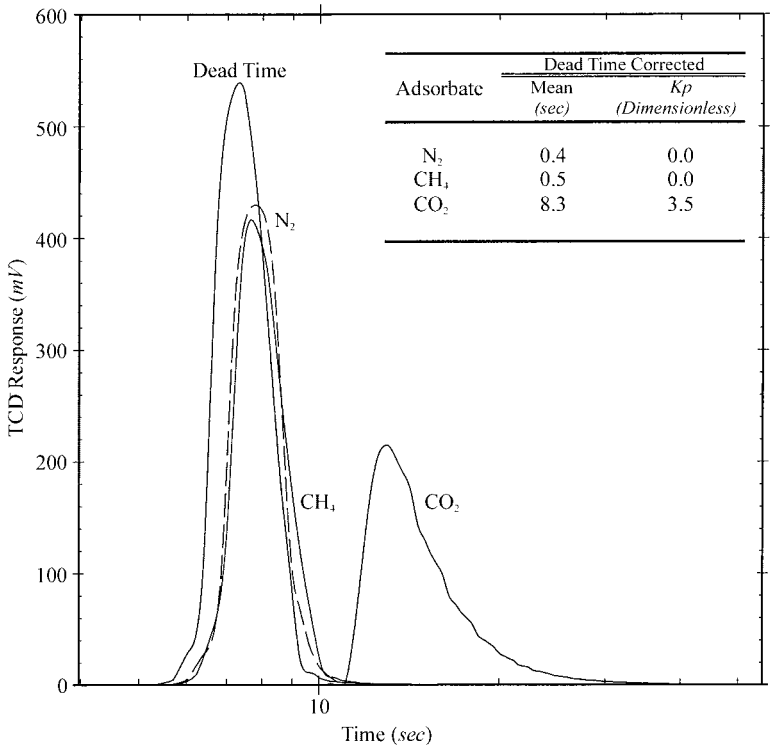

Figure 2. TCD responses for Kaolin binder.

MARCEL DEKKER, INC.
270 Madison Avenue, New York, New York 10016

NUMERICAL METHODS

In order to determine the parameters for the pure component fits to the Freundlich, Langmuir, Nitta, and VST isotherm forms, a non-linear regression was performed using a modified Levenberg–Marquardt algorithm with a finite difference Jacobian. To find the optimal values of the B_i and C_i parameters in Eq. (23) a non-linear constrained optimization technique was used. This was based on a Generalized Reduced Gradient (GRG2) nonlinear optimization code. Quadratic extrapolation was employed to obtain initial estimates of the basic variables in each one-dimensional search. The Jacobian for the objective and constraint functions were approximated by a central finite difference approach. A quasi-Newton iteration method was also used. Tolerance and convergence were each set at 10^{-6}. The solution was taken when no further change in Eq. (23) could be

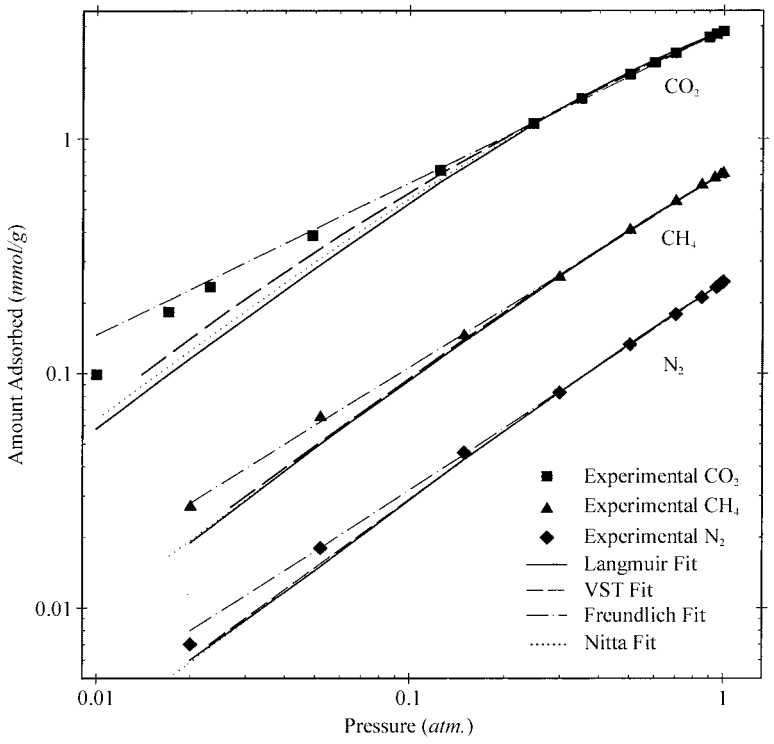

Figure 3. Experimental pure gas isotherms for CO_2, N_2 and CH_4 with H-ZSM-5-30 at 40°C with their corresponding Langmuir, Freundlich, Nitta and VST fit.

MARCEL DEKKER, INC.
270 Madison Avenue, New York, New York 10016

obtained for a wide range of starting values. This wide range of initial guesses ensured that the absolute and not the local minimum was obtained.

RESULTS

Kaolin Binder

The Kaolin binder was tested for adsorption characteristics at 0% loading with CO_2, CH_4 and N_2, at the conditions used in this study. Pure Kaolin was pelletized into 20–60 mesh and was packed into the adsorption column. It was then regenerated at 350°C for 12 hr under a 40 *cc*/min (at 40°C) He purge. Injections of each of the adsorbates studied were then performed and response noted. The results of the analysis are shown in Fig. 2. The dead time response of

Table 4. Experimental and Prediction Data for Pure CO_2 with H-ZSM-5-30

Pressure (atm)		Amount Adsorbed (mmol/g)		
Experimental	FH-VST	Experimental	Langmuir	FH-VST
0.000	0.000	0.000	0.000	0.000
0.010	0.014	0.099	0.058	0.099
0.017	0.026	0.183	0.099	0.183
0.023	0.034	0.234	0.133	0.234
0.049	0.060	0.387	0.275	0.387
0.125	0.131	0.735	0.652	0.735
0.247	0.243	1.161	1.154	1.161
0.350	0.346	1.481	1.504	1.481
0.500	0.497	1.877	1.924	1.877
0.600	0.598	2.106	2.158	2.106
0.700	0.697	2.310	2.363	2.310
0.899	0.900	2.687	2.706	2.687
0.950	0.955	2.780	2.781	2.780
1.000	0.999	2.852	2.852	2.852
	$SSR = 4.637 \times 10^{-4}$	—	4.721×10^{-2}	—

Parameters	
Langmuir	FH-VST
$B = 1.0724$	$b = 7.6382$
$q_m = 5.5117$	$a_{1v} = 2.7325$
	$q_m^{\infty} = 18.3357$

MARCEL DEKKER, INC.
270 Madison Avenue, New York, New York 10016

the system is also shown, with respect to the Kaolin packed column. The data shown in Fig. 2 confirms that the contribution of the binder to the adsorption characteristics is negligible for N_2 and CH_4. The binder does have an effect on the adsorption characteristics of CO_2. However, magnitude of this contribution is negligible in comparison to the values obtained with the adsorbent + binder. Further, the contribution of the binder will decrease as the carrier composition of each of the adsorbates is increased. Therefore, the Kaolin binder is considered as inert filler, under the conditions used in this study.

Pure Isotherms

Pure gas isotherms for CO_2, N_2 (6) and CH_4 (7) with H-ZSM-5-30 at 40°C are shown in Fig. 3 as a log–log plot. The best fit curves representing Langmuir, Nitta, Freundlich and VST isotherm forms for CO_2, CH_4, and N_2 are also shown in this figure. All the models fit the data well at the high-pressure region;

Table 5. Experimental and Prediction Data for Pure CH_4 with H-ZSM-5-30

Pressure (atm)		Amount Adsorbed (mmol/g)		
Experimental	FH-VST	Experimental	Langmuir	FH-VST
0.000	0.000	0.000	0.000	0.000
0.020	0.027	0.027	0.019	0.027
0.052	0.067	0.065	0.050	0.065
0.149	0.155	0.145	0.137	0.145
0.299	0.291	0.257	0.260	0.257
0.501	0.496	0.407	0.409	0.407
0.702	0.701	0.540	0.540	0.540
0.852	0.858	0.634	0.627	0.634
0.937	0.940	0.680	0.674	0.680
0.979	0.980	0.702	0.696	0.702
1.000	0.994	0.710	0.707	0.710
	$SSR = 4.605 \times 10^{-4}$	—	5.060×10^{-4}	—

Parameters	
Langmuir	FH-VST
$B = 0.3670$	$b = 1.0076$
$q_m = 2.6339$	$a_{1v} = 2.1651$
	$q_m^{\infty} = 10.5767$

MARCEL DEKKER, INC.
270 Madison Avenue, New York, New York 10016

however, the Freundlich isotherm fits represent the experimental data with the most accuracy in the low-pressure region. The pure component data for CO_2, CH_4, and N_2, with the curve fit values and regressed parameters are given in Tables 4–6, respectively.

The pure isotherms were found by first regenerating the adsorbent, then proceeding with an adsorption run, then purge desorption run, then adsorption run again for various compositions of y_1. The desorption was performed by lowering the mole fraction in the carrier gas from 100% down to 0% in steps and injecting samples after attaining equilibrium after each concentration change. Equilibrium of the new carrier gas composition with the adsorbent was confirmed by noting that the change in the K_p values at a given y_1 composition would converge as equilibrium was approached. When equilibrium was reached, a final series of injections were performed and the average K_p value was determined before y_1 was lowered again. The pure isotherms were then obtained by the integration of Eq. (4) by using the values of experimentally determined K_P values at different y_1.

Table 6. Experimental and Prediction Data for Pure N_2 with H-ZSM-5-30

Pressure (atm.)		Amount Adsorbed (mmol/g)		
Experimental	FH-VST	Experimental	Langmuir	FH-VST
0.000	0.000	0.000	0.000	0.000
0.020	0.023	0.007	0.006	0.007
0.052	0.061	0.018	0.015	0.018
0.149	0.160	0.046	0.043	0.046
0.299	0.300	0.083	0.083	0.083
0.501	0.500	0.133	0.134	0.133
0.702	0.696	0.179	0.181	0.179
0.852	0.844	0.211	0.213	0.211
0.949	0.947	0.233	0.234	0.233
0.979	0.982	0.241	0.240	0.241
1.000	1.007	0.246	0.244	0.246
	$SSR = 3.824 \times 10^{-4}$	—	2.911×10^{-5}	—

Parameters	
Langmuir	FH-VST
$B = 0.2063$	$b = 0.2967$
$q_m = 1.4266$	$a_{1v} = 2.1536$
	$q_m^{\infty} = 6.6874$

MARCEL DEKKER, INC.
270 Madison Avenue, New York, New York 10016

For the H-ZSM-5-30 adsorbent the adsorption capacity for each of the adsorbates vary in magnitude, where the capacity decreased in the following order: $CO_2 \gg CH_4 > N_2$. The pore opening and channel structure of H-ZSM-5-30 is large enough to neglect any steric effects of the adsorbates with the adsorbent structure. However, the cationic nature of the adsorbent surface is predominantly the cause of the differences in adsorption capacity. Carbon dioxide possesses a large quadrupole moment (Table 3). This quadrupole moment produces a strong attraction to the electrostatic field of the cationic site, and results with the high capacity (26).

Methane has a high degree of polarizibility. This property, when in close proximity to the cation within the structure causes a momentary shift in the time averaged neutral electrostatic field of CH_4. This induced polarity causes an attraction to the adsorbent surface.

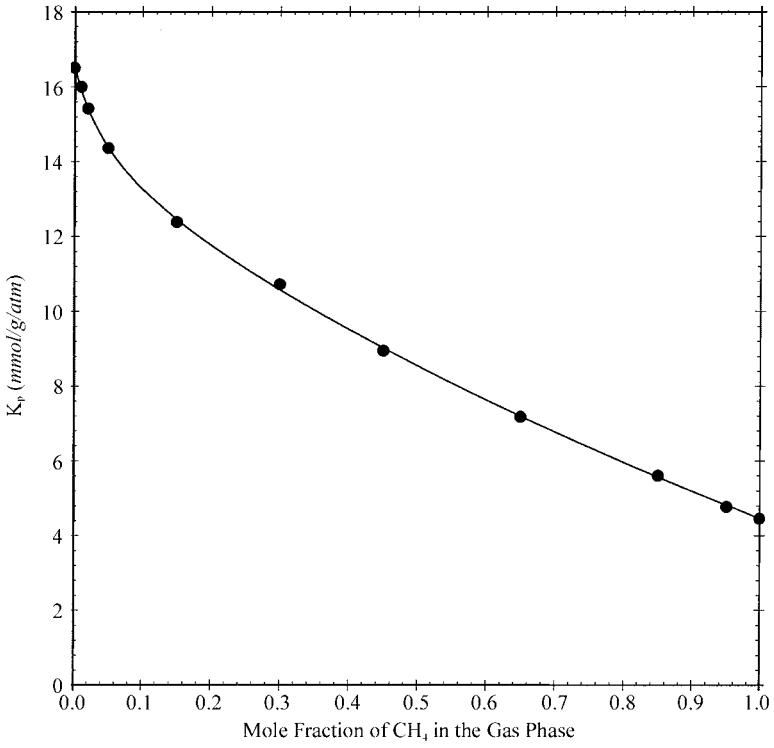

Figure 4. Experimental CH_4–N_2 binary K_p data and the resulting form of Eq. (22) as determined from the HT-CPM solution method.

MARCEL DEKKER, INC.
270 Madison Avenue, New York, New York 10016

Nitrogen also possesses a quadrupole moment, but it is much lower in magnitude than CO_2's. Nitrogen's polarizibility is also lower than that of CO_2 and CH_4. These properties contribute to the low capacity of the adsorbent for nitrogen.

Binary CH_4-N_2 System

The experimental CH_4-N_2 binary K_p data and the resulting form of Eq. (22) (as determined from the HT-CPM solution method) are shown in Fig. 4. The sudden drop of the data at $y_1 < 5\%$ CH_4 mole fraction in the gas phase shows that the adsorption is slightly competitive for the accessible cationic sites. This was also the trend observed in our previous work with CO_2-N_2 and the CO_2-CH_4 binary systems (6,7).

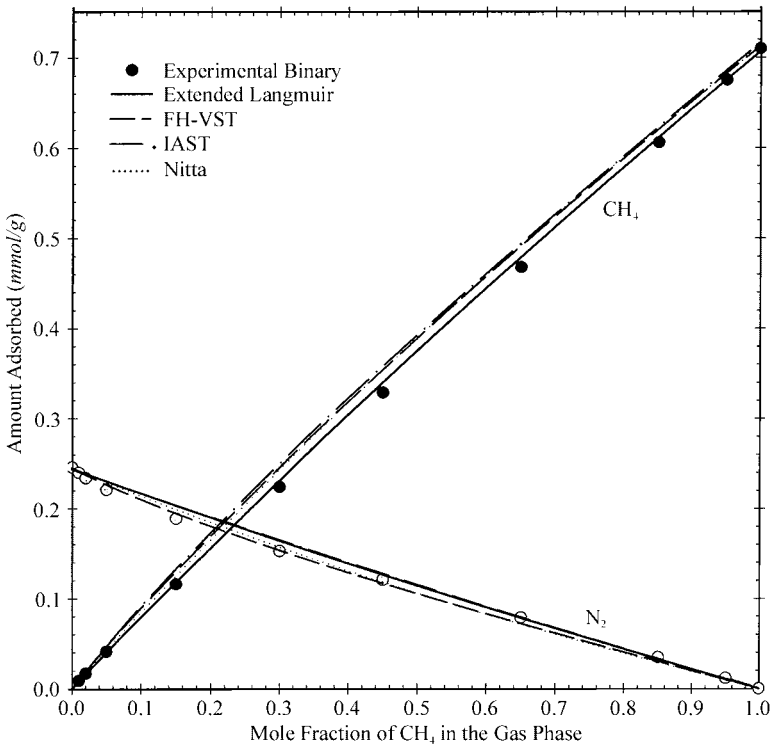

Figure 5. Experimental and predicted binary isotherms for CH_4-N_2 gas mixtures with H-ZSM-5-30 as the adsorbent at 40°C and 1.0 atm total pressure.

From this K_p data, the binary isotherms were determined with the HT-CPM. The solution determined the B_i and C_i parameters that were used with Eqs. (20) and (21) to define the binary isotherms shown in Fig. 5 as experimental binary data points. The CH_4 binary isotherm exhibits a nearly perfect linear trend at all CH_4 mole fractions. This suggests that the adsorption is occurring in the Henry's Law region for this adsorbate. However, the N_2 isotherm is not linear and exhibits concavity at low CH_4 mole fractions, which is characteristic of competitive adsorption. This competitive adsorption mainly occurs at low CH_4 mole fractions in the feed, which suggests that the two adsorbates are attempting to occupy the same active cationic adsorption site. Methane possesses a much higher degree of polarizability than N_2 and this property difference allows CH_4 to occupy those cationic sites over N_2. However, the binary CH_4 isotherm does not show any convexity or concavity. This suggests that the CH_4 in the pores occupies the cationic sites first, but not completely. If full coverage of the cations

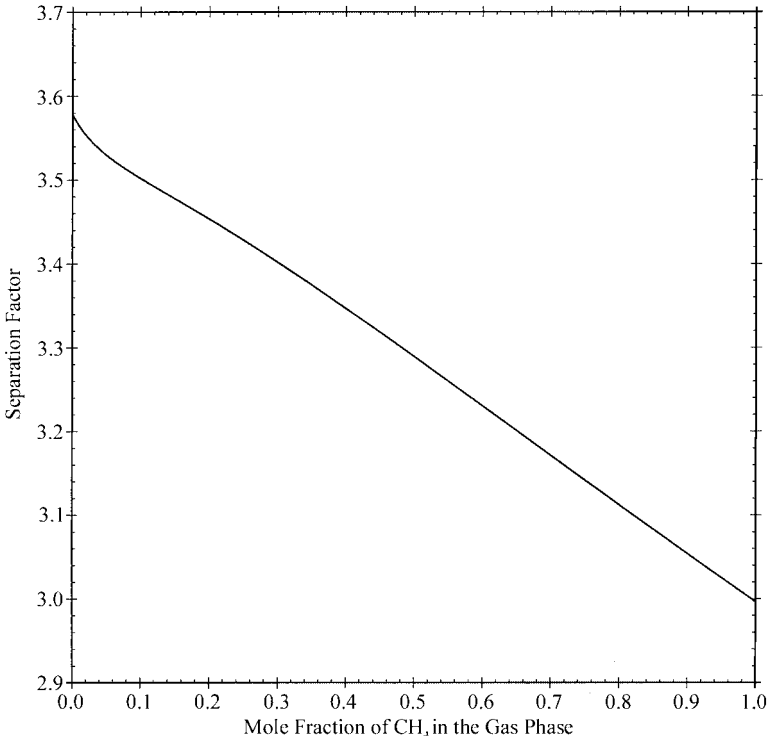

Figure 6. Separation factors as a function of y_1 for CH_4–N_2 binary system with H-ZSM-5-30 at 40°C.

MARCEL DEKKER, INC.
270 Madison Avenue, New York, New York 10016

were achieved, then the isotherm would exhibit a degree of convexity at low CH_4 mole fractions, owing to the high degree of uptake on these sites.

The separation factor, defined by Eq. (24), is shown as a function of y_1 in Fig. 6 for CH_4–N_2 binary system. The maximum separation factor (3.58) occurs at the limit as $y_1 \rightarrow 0$ and the minimum (2.97) is at the limit as $y_1 \rightarrow 1$. From this data, it can be concluded that the H-ZSM-5-30 adsorbent is not selective enough to be considered as an economically viable adsorbent at the conditions used in this work.

THEORETICAL PREDICTIONS

There are a vast number of multi-component predictive models available in the literature. For this study, the Extended Langmuir (EL), Extended Nitta

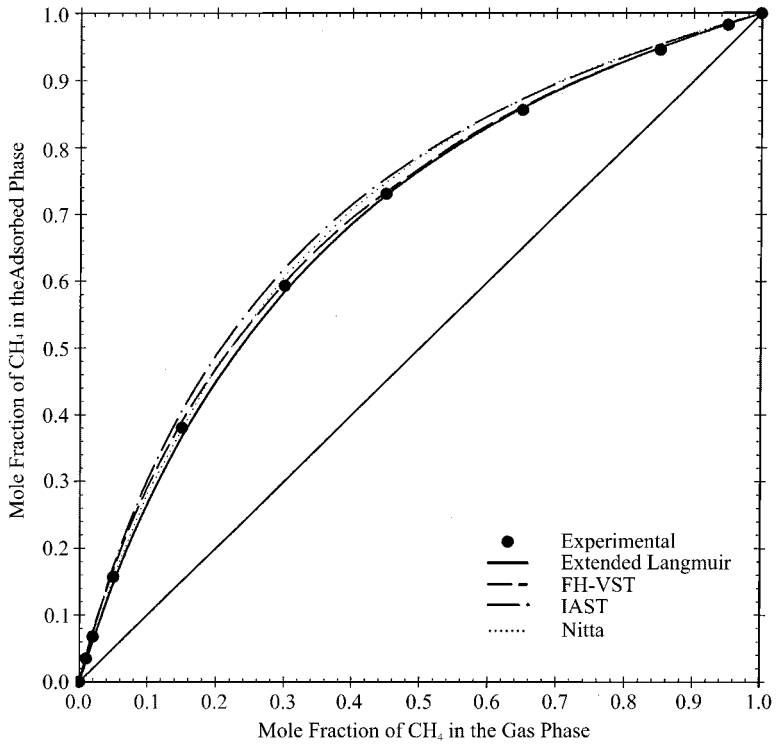

Figure 7. Experimental and predicted x–y adsorption phase diagrams for CH_4–N_2 binary system with H-ZSM-5-30 at 40°C.

(Nitta), Ideal Adsorbed Solution Theory (IAST) and the Vacancy Solution Theory (VST) were chosen. For the IAST calculations, Freundlich isotherm fits were used to represent the pure component data. With the VST, the activity coefficients can be modeled with several forms. For this work, the Flory–Huggins form for the activity coefficients was used (FH-VST).

CH_4–N_2 Binary Predictions

The experimental binary isotherms and predictions using each of previously mentioned models are shown in Fig. 5 for CH_4–N_2 gas mixtures with H-ZSM-5-30 as the adsorbent at 40°C and 1.0 atm total pressure. All the

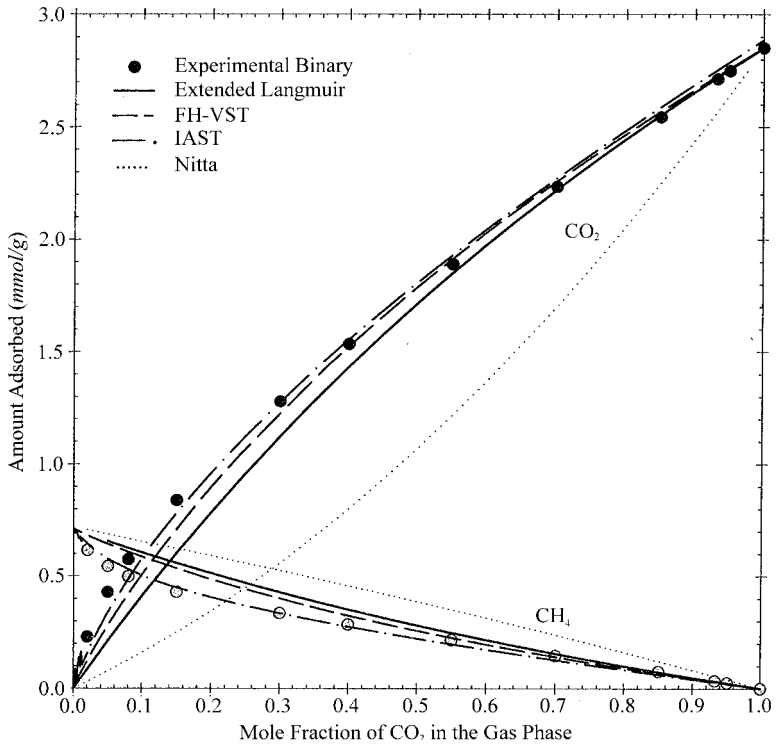

Figure 8. Experimental and predicted binary isotherms for CO_2–CH_4 gas mixtures with H-ZSM-5-30 as the adsorbent at 40°C and 1.0 atm total pressure.

models predict the data reasonable well. The FH-VST model predicts the slightly competitive adsorption for N_2 at low CH_4 mole fractions. The Extended Langmuir model predicts the CH_4 binary isotherm most accurately among the models used. Any of the models could be applied to this system within a certain degree of accuracy.

The $x-y$ adsorption phase diagram is shown in Fig. 7 for the CH_4-N_2 binary system. Again, all the models are capable of predicting the behavior of this binary system reasonably well. The CH_4-N_2 binary system with H-ZSM-5-30 does not exhibit strong competitive adsorption. In addition, the capacity of the adsorbent for these components is not very high. These characteristics translate into an adsorption system that is relatively easy to predict since the binary adsorption behavior closely follows the same trends as the pure component adsorption.

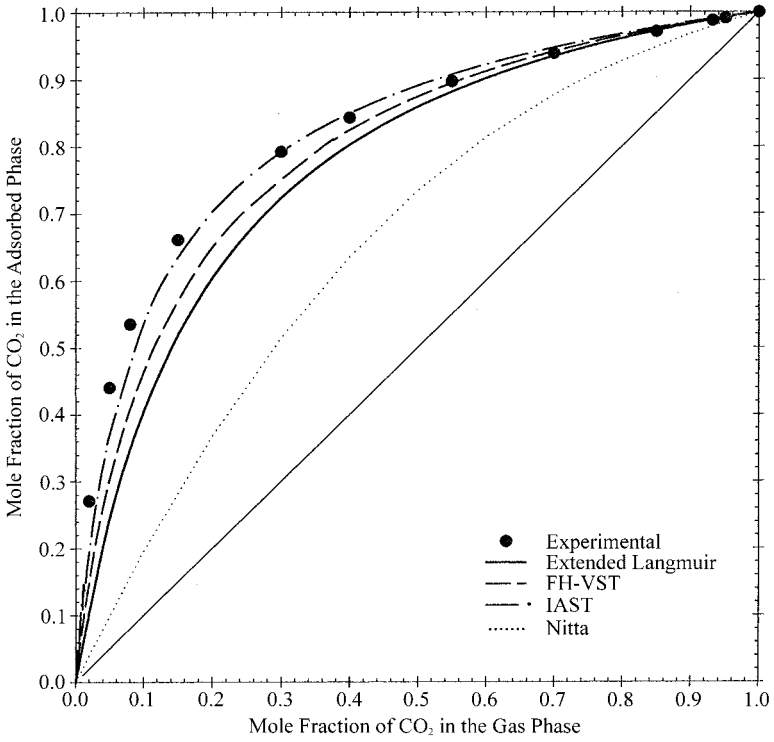

Figure 9. Experimental and predicted $x-y$ adsorption phase diagrams for CO_2-CH_4 binary system with H-ZSM-5-30 at 40°C.

MARCEL DEKKER, INC.
270 Madison Avenue, New York, New York 10016

CO_2-CH_4 Binary Predictions

The experimental binary isotherms (7) and predictions using each of previously mentioned models are shown in Fig. 8 for the CO_2-CH_4 gas mixtures with H-ZSM-5-30 as the adsorbent at 40°C and 1.0 atm total pressure. The rapid drop in the CH_4 isotherm at low CO_2 mole fractions is largely due to the dominant CO_2 adsorption in this region. The IAST predicts the binary isotherms most accurately among the models used. Extended Nitta does not predict the binary isotherms at all and should not be used for this system. The reason for that is the unreasonably high value of a (= 9.852) for CO_2. This value represents the number of adsorption sites that the CO_2 molecule would occupy in the ZSM-5. Considering the size of the CO_2 molecule and the pore size of ZSM-5, the value of 9.852 does not make sense physically, although the pure component isotherm fit for Nitta model is a reasonable one.

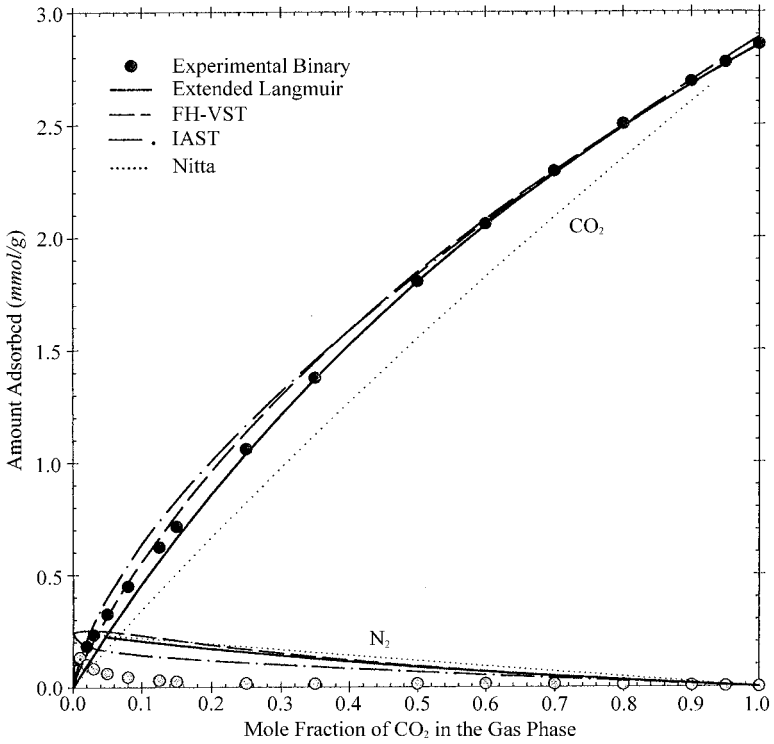

Figure 10. Experimental and predicted binary isotherms for CO_2-N_2 gas mixtures with H-ZSM-5-30 as the adsorbent at 40°C and 1.0 atm total pressure.

The $x-y$ adsorption phase diagram is shown in Fig. 9. Again, the IAST is the most capable of predicting the behavior of this binary system. Extended Nitta is the worst one and should not be used for the prediction of this system.

CO_2-N_2 Binary Predictions

The experimental binary isotherms (7) and predictions using each of previously mentioned models are shown in Fig. 10 for the CO_2-N_2 with H-ZSM-5-30 as the adsorbent at 40°C and 1.0 atm total pressure. None of the models predicts the N_2 binary isotherm accurately. This is largely due to the very dominant electrostatic properties of CO_2 controlling adsorption on the active adsorption cationic sites and the pore walls. The models do not account for the dominant adsorption of one of the adsorbates. This results in close to linear

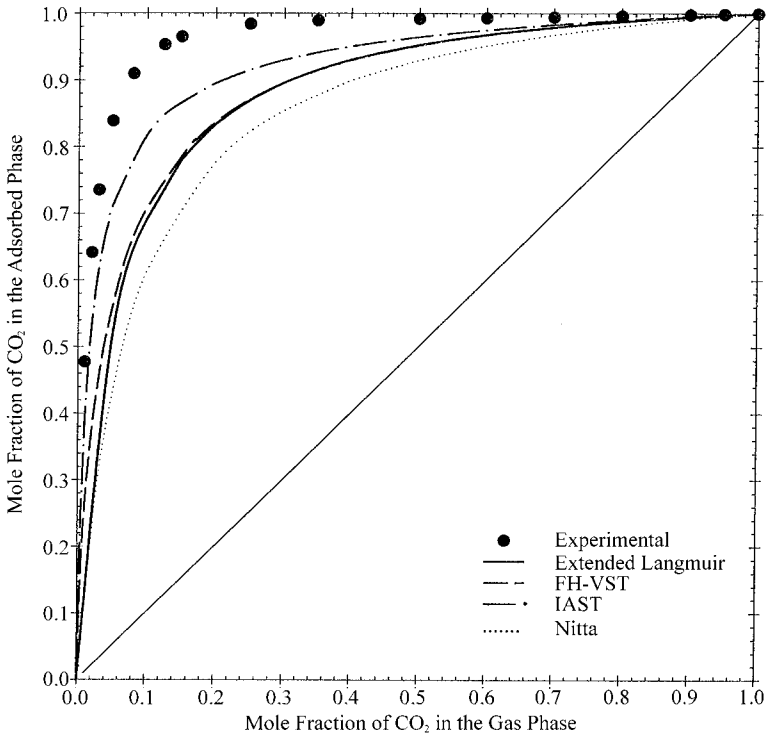

Figure 11. Experimental and predicted $x-y$ adsorption phase diagrams for CO_2-N_2 binary system with H-ZSM-5-30 at 40°C.

prediction for the N_2 isotherm for all the models, and reasonably accurate prediction of the CO_2 isotherm, except the Extended Nitta. The accuracy of the prediction for different models varies depending on the range of concentration in the gas phase. EL predicts the CO_2 binary isotherm accurately for CO_2 concentrations higher than 20%. FH-VST predicts the CO_2 isotherm well at low and high CO_2 concentrations, but not in the intermediate concentration range. IAST over-predicts the CO_2 isotherm at low CO_2 concentration, whereas Extended Nitta does not predict the CO_2 isotherm well. Sircar (18) discussed the problems with the applicability of the IAST model for different size adsorbates and different degrees of heterogeneity for adsorption.

The $x-y$ adsorption phase diagram is shown in Fig. 11. Again, none of the models are capable of predicting this binary system behavior. That much discrepancy between the experimental results and the predictions come from the fact that N_2 binary isotherm is not predicted well at all by any of the models used. Since Extended Nitta did not predict CO_2 adsorption well, either, this model was the worst one to predict the $x-y$ diagram and should not be used for this system.

For this binary system, CO_2 is very dominant and controls the adsorption on the cationic sites within the structure, as shown by the binary isotherms in Fig. 10. This type of behavior is not predicted well by the models used in this work. Therefore, when one component is strongly adsorbed and the other component is weakly adsorbed, the models do not predict the adsorption behavior of the weakly adsorbed component well.

CONCLUSIONS

The adsorption of binary gas mixtures of CO_2-N_2, CO_2-CH_4, and CH_4-N_2 were studied by using H-ZSM-5 as the adsorbent with a SiO_2/Al_2O_3 ratio of 30. Pure isotherms for N_2 and CH_4 at 40°C and CH_4-N_2 binary isotherms at 40°C and 1.0 atm total pressure have been determined experimentally using concentration pulse chromatography. The Extended Langmuir Model, Extended Nitta, Ideal Adsorbed Solution Theory and the Flory–Huggins form of the Vacancy Solution Theory were used to predict the binary isotherms for the CH_4-N_2, CO_2-CH_4 and CO_2-N_2 systems at 40°C and 1.0 atm total pressure. These predictions were compared to the experimental binary data obtained with HT-CPM.

The following conclusions have been reached:

- The HT-CPM was applied to the K_p vs. concentration data for the CH_4-N_2 adsorption system, which expanded this method's applicability.
- The CH_4-N_2 binary system exhibited slightly competitive adsorption at low CH_4 mole fractions in the feed.

MARCEL DEKKER, INC.
270 Madison Avenue, New York, New York 10016

The separation factor for the CH_4-N_2 system showed a steady decline from 3.58 to 2.97 with increasing CH_4 mole fractions in the feed.

For CH_4-N_2 binary system, Extended Langmuir Model predictions were the closest to the experimental data for CH_4 behavior, whereas FH-VST was the best to predict the N_2 behavior.

The IAST was the model most accurately predicted CH_4-CO_2 binary adsorption behavior.

None of the models were capable of predicting the adsorption of CO_2-N_2 binary system across the entire range of mole fractions.

The interaction of the heterogeneous nature of the adsorbent surface and the adsorbates was not fully accounted for by any of the predictive models.

When one component is strongly adsorbed and the other component is very weakly adsorbed the models do not accurately predict the binary adsorption behavior.

NOMENCLATURE

A,B,C	Parameters (mmo1/g/atm)
b	Herny's Law Constant (Eq. 26 and 27) (mmo1/g/atm)
B	Herny's Law Constant (Eq. 25 and 28) (1/atm)
c	Concentration measured as voltage (mV)
CF	Conversion factor (mmol/g/atm)
D	Constant in Eq. (4) (mmol/g/atm)
f,g,h	Function
K	Effective isotherm slope (Dimensionless)
K_p	Effective iostherm slope (mmol/g/atm)
L	Length of the column (m)
P	Pressure (atm.)
q	Amount adsorbed (mmol/g)
q_m	Monolayer amount adsorbed (mmol/g)
q_m^{∞}	Limiting amount adsorbed (mmol/g)
t	Time (sec)
x	Mole fraction in the adsorbed phase (Dimensionless)
y	Mole fraction in the gas phase (Dimensionless)

Greek letters

α	Separation factor (Dimensionless)
α_{1v}	Component interaction parameter (Dimensionless)
λ	Parameter in Eq. (17) (Dimensionless)
ϵ	Bed porosity (Dimensionless)

MARCEL DEKKER, INC.
270 Madison Avenue, New York, New York 10016

μ Mean retention time (sec)
ν Interstitial velocity (m/sec)
θ Coverage (q/q_m^{∞}) (Dimensionless)

Subscripts
1 Component 1
2 Component 2
Max Maximum
Min Minimum
i index

ACKNOWLEDGMENTS

Financial support received from the Natural Sciences and Engineering Research Council (NSERC) of Canada is gratefully acknowledged. ZSM-5 samples were prepared and donated by Dr Ahmet Sirkecioglu of the Department of Chemical Engineering at Istanbul Technical University in Turkey.

REFERENCES

1. Farla, J.C.M.; Hendriks, C. A.; Blok, K. Carbon Dioxide Recovery From Industrial Processes. Energy Conv. Mgmt **1995**, *36* (6–9), 827–830.
2. Shah, D.B.; Ruthven, D.M. Measurement of Zeolitic Diffusivities by Chromatography. AIChE J. **1977**, *23* (6), 804–810.
3. Van der Vlist, E.; Van der Meijden, J. Determination of the Adsorption Isotherms of the Components of Binary Gas Mixtures by Gas Chromatography. J. Chromatogr. **1973**, *79*, 1–13.
4. Hyun, S.H.; Danner, R.P. Determination of Gas Adsorption Equilibria by the Concentration-Pulse Technique. AIChE Symp. Ser. **1982**, *78* (219), 19–28.
5. Tezel, F.H.; Tezel, H.O.; Ruthven, D.M. Determination of Pure and Binary Isotherms for Nitrogen and Krypton. J. Colloid Interface Sci. **1992**, *149* (1), 197–207.
6. Harlick, P.J.E.; Tezel, F.H. A Novel Solution Method for Interpreting Binary Adsorption Isotherms from Concentration Pulse Chromatography Data. Adsorption **2000**, *6*, 293–309.
7. Harlick, P.J.E.; Tezel, F.H. CO_2–N_2 and CO_2–CH_4 Binary Adsorption Isotherms with H-ZSM-5: The Importance of Experimental Data Regression with the Concentration Pulse Method. Can. J. Chem. Engng **2001**, *79*, 236–245.

8. Triebe, R.W.; Tezel, F.H. Adsorption of Nitrogen and Carbon Monoxide on Clinoptilolite: Determination and Prediction of Pure and Binary Isotherms. Can. J. Chem. Engng **1995**, *73*, 717–724.
9. Harlick, P.J.E.; Tezel, F.H. Use of Concentration Pulse Chromatography for Determining Binary Adsorption Isotherms. Presented at the Annual Meeting of the American Institute of Chemical Engineering in Los Angeles, U.S.A. **2000**.
10. Schneider, P.; Smith, J.M. Adsorption Rate Constants from Chromatography. AIChE J. **1968**, *14* (5), 762–771.
11. Schneider, P.; Smith, J. M. Chromatographic Study of Surface Diffusion. AIChE J. **1968**, *14* (6), 886–895.
12. Ruthven, D.M.; Kumar, R. An Experimental Study of Single-Component and Binary Adsorption Equilibria by a Chromatographic Method. Ind. Eng. Chem. Fundam. **1980**, *19*, 27–32.
13. Hyun, S.H.; Danner, R.P. Gas Adsorption Isotherms by use of Perturbation Chromatography. Ind. Eng. Chem. Fundam. **1985**, *24*, 95–101.
14. Calleja, G.; Pau, J.; Calles, J.A. Pure and Multicomponent Adsorption Equilibrium of Carbon Dioxide, Ethylene and Propane on ZSM-5 Zeolites with Different Si/Al Ratios. J. Chem. Eng. Data **1998**, *43*, 994–1003.
15. Yang, R.T. *Gas Separation by Adsorption Processes*; Butterworth Publishers: Mass., U.S.A., 1987.
16. Ruthven, D.M. *Principles of Adsorption and Adsorption Processes*; John Wiley & Sons Inc. New York, U.S.A., 1984.
17. Nitta, T.; Shigetomi, T.; Kuro-oka, M.; Katayama, T. An Adsorption Isotherm of Multi-Site Occupancy Model for Homogeneous Surface. J. Chem. Eng. Jpn **1984**, *17*, 39.
18. Sircar, S. Influence of Adsorbate Size and Adsorbent Heterogeneity on IAST. AIChE J. **1995**, *41* (5), 1134–1145.
19. Myers, A.L.; Prausnitz, J.M. Thermodynamics of Mixed Gas Adsorption. AIChE J. **1965**, *11*, 121.
20. Cochran, T.W.; Kabel, R.L.; Danner, R.P Vacancy Solution Theory of Adsorption Using Flory–Huggins Activity Coefficient Equations. AIChE J. **1985**, *31* (2), 268–277.
21. Cochran, T.W.; Kabel, R.L.; Danner, R.P. The Vacancy Solution Model of Adsorption—Improvements and Recommendations. AIChE J. **1985**, *31* (12), 2075–2082.
22. Suwanayuen, S.; Danner, R.P. A Gas Adsorption Isotherm Equation Based on Vacancy Solution Theory. AIChE J. **1980**, *26* (1), 68–76.
23. Suwanayuen, S.; Danner, R.P. Vacancy Solution Theory of Adsorption from Gas Mixtures. AIChE J. **1980**, *26* (1), 76–83.

MARCEL DEKKER, INC.
270 Madison Avenue, New York, New York 10016

24. Yamazaki, T.; Katoh, M.; Ozawa, S.; Ogino, Y. Adsorption of CO_2 over Univalent Cation-Exchanged ZSM-5 Zeolites. Mol. Phys. **1993**, *80* (2), 313–324.
25. Saito, A.; Foley, H.C. High-Resolution Nitrogen and Argon Adsorption on ZSM-5 Zeolites: Effects of Cation Exchange and Si/Al Ratio. Microporous Mater. **1995**, *3* (4), 1995.
26. Huang, Y.Y. Quadruple Interaction of Carbon Dioxide on Silica–Alumina Surface. J. Phys. Chem. **1973**, *77* (1), 103–106.
27. Golden, T.C.; Sircar, S. Gas Adsorption on Silicalite. J. Colloid Interface Sci. **1994**, *162*, 182–188.

Received May 2000
Revised April 2001

Request Permission or Order Reprints Instantly!